ISPRS Journal of Photogrammetry and Remote Sensing 108 (2015) 151–160

Contents lists available at ScienceDirect

ISPRS Journal of Photogrammetry and Remote Sensing

journal homepage: www.elsevier.com/locate/isprsjprs

Sensitivity analysis of vegetation indices to drought over two tallgrass prairie sites

Rajen Bajgain [a], Xiangming Xiao [a,b,*], Pradeep Wagle [a], Jeffrey Basara [c,d], Yuting Zhou [a]

[a] Department of Microbiology and Plant Biology, Center for Spatial Analysis, University of Oklahoma, Norman, OK, USA
[b] Institute of Biodiversity of Sciences, Fudan University, Shanghai 200433, China
[c] School of Meteorology, University of Oklahoma, Norman, OK, USA
[d] Oklahoma Climatological Survey, Norman, OK, USA

ARTICLE INFO

Article history:
Received 25 March 2015
Received in revised form 16 July 2015
Accepted 16 July 2015

Keywords:
Drought
Drought intensity
Soil moisture
Tallgrass prairie
Vegetation indices

ABSTRACT

Vegetation growth is one of the important indicators of drought events. Greenness-related vegetation indices (VIs) such as Normalized Difference Vegetation Index (NDVI) and Enhanced Vegetation Index (EVI) are often used for the assessment of agricultural drought. There is a need to evaluate the sensitivity of water-related vegetation indices such as Land Surface Water Index (LSWI) to assess drought and associated impacts. Moderate-Resolution Imaging Spectroradiometer (MODIS) derived time series NDVI, EVI and LSWI data during 2000–2013 were compared for their sensitivity to drought at two tallgrass prairie sites in the Oklahoma Mesonet (Marena and El Reno). Each site has continuous soil moisture measurements at three different depths (5, 25 and 60 cm) and precipitation data for the study period (2000–2013) at 5-min intervals. As expected, averaged values of vegetation indices consistently lower under drought conditions than normal conditions. LSWI decreased the most in drought years (2006, 2011 and 2012) when compared to its magnitudes in pluvial years (2007, 2013), followed by EVI and NDVI, respectively. Because green vegetation has positive LSWI values (>0) and dry vegetation has negative LSWI values (<0), much longer durations of LSWI < 0 were found in the summer periods of drought years rather than in pluvial years. A LSWI-based drought severity scheme ($LSWI > 0.1$; $0 < LSWI \leqslant 0.1$; $-0.1 < LSWI \leqslant 0$; $LSWI \leqslant -0.1$) corresponded well with the drought severity categories (0; D0; D1: D2; D3 and D4) defined by the United States Drought Monitor (USDM) at these two study sites. Our results indicate that the number of days with LSWI < 0 during the summer and LSWI-based drought severity scheme can be simple, effective and complementary indicator for assessing drought in tallgrass prairie grasslands at a 500-m spatial resolution.

1. Introduction

Drought is a recurring event of Oklahoma's climate cycle (Basara et al., 2013; Christian et al., 2015) and poses significant impacts on various sectors of the economy (OWRB, 2010). Seasonal drought can occur at any time of the year and the summer drought that coincides with the growing season can cause ecological imbalances and influences surface biophysical parameters such as vegetation indices, land surface temperature, soil moisture and evapotranspiration (Ghulam et al., 2007; Reichstein et al., 2002). This ultimately impacts the productivity of the tallgrass prairie ecosystem, which can cause billions of dollars in damage to livestock's industries depending on its timing, duration and severity.

Several conceptual definitions of drought have been classified into four major categories: meteorological, agricultural, hydrological and socio-economic droughts (Wilhite and Glantz, 1985). Understanding the need to quantify drought severity, researchers have developed several methods to assess and diagnose different droughts. Meteorological drought indices (Rainfall Anomaly Index, Bhalme and Mooley Drought Index, Drought Severity Index, Standardized Precipitation Index) were solely based on meteorological data such as precipitation and temperature (Bhalme et al., 1981; McKee et al., 1993; Van Rooy, 1965). Agricultural drought indices (Crop Moisture Index, the Soil moisture Drought Index, Soil Moisture Deficit Index) considered soil

* Corresponding author at: 101 David L. Boren Blvd, Norman, OK 73019, USA. Tel.: +1 405 325 8941; fax: +1 405 325 3442.
E-mail address: xiangming.xiao@ou.edu (X. Xiao).

http://dx.doi.org/10.1016/j.isprsjprs.2015.07.004
0924-2716/

moisture and evapotranspiration deficit (Hollinger et al., 1993; Narasimhan and Srinivasan, 2005; Palmer, 1965), while hydrological drought indices (Palmer Hydrological Drought Index, Surface Water Supply Index, Reclamation Drought Index) were based on a water balance model (Shafer and Dezman, 1982; Weghorst, 1996).

With the advancement of Earth observations from satellite-based sensors, numerous recent studies have used remote sensing data for assessing drought impacts (Ghulam et al., 2007; Peters et al., 2002; Tadesse et al., 2005; Wan et al., 2004). Over the period of more than 20 years, a number of remote sensing based vegetation indices (VIs) have been developed from various spectral band combinations to monitor vegetation (Table 1). While greenness-related VIs retrieved from remote sensing land surface reflectance such as Normalized Difference Vegetation Index (NDVI) and Enhanced Vegetative Index (EVI) have often been used for vegetation condition monitoring (Diodato and Bellocchi, 2008; Herrmann et al., 2005; Song and Ma, 2011), NDVI derived indices such as Anomaly Vegetation Index (Weiying et al., 1994) and the Vegetation Condition Index (VCI) (Kogan, 1995) were used to relate vegetation dynamics to drought patterns. Similarly, several water related satellite-based vegetation indices that estimate vegetation water content have been used for drought detection (Chen et al., 2005; Fensholt and Sandholt, 2003; Gao, 1996; Kimes et al., 1981). Shortwave infrared reflectance (SWIR) and leaf water content are negatively related due to the large absorption (Hunt and Rock, 1989; Tucker, 1980) and is contrasted with near infrared (NIR) band to normalize the effects of other leaf parameters such as internal leaf structure for proper estimation of vegetation water content (Ceccato et al., 2001; Gao, 1996). Based on the analysis of reflectance spectra, combination of SWIR and NIR bands have been reported by numerous studies under different names: Normalized Difference of Landsat TM bands 4 and 5, ND45 (Kimes et al., 1981); Normalized Difference Infrared Index, NDII (Hardisky et al., 1983); Shortwave Water Stress Index, SWIS (Fensholt and Sandholt, 2003); Normalized Difference Water Index, NDWI (Jackson et al., 2004; Maki et al., 2004) and Land Surface Water Index, LSWI (Qin et al., 2015; Xiao et al., 2002; Zhang et al., 2015). These indices have proven to be effective in monitoring the water content of vegetation. However, NDVI has been the most popular and extensively used satellite-based index for drought monitoring over the past decades. Numerous studies have analyzed the relationships between NDVI and rainfall across geographical areas and vegetation types (Bhalme et al., 1981; Boschetti et al., 2013; McKee et al., 1993; Van Rooy, 1965). In the central and northern Great Plains grasslands, growing season rainfall, growing degree days and potential evapotranspiration exerted strong control over grassland productivity (Yang et al., 1998). There was a stronger relationship between NDVI and rainfall than between NDVI and temperature for the grassland located in the central and northern Great Plains of the US (Wang et al., 2001). Like other drought monitoring algorithms (Ji and Peters, 2003; Liu and Kogan, 1996; Nemani and Running, 1989; Pettorelli et al., 2005), the Vegetation Drought Response Index (VegDRI) introduced by the United States Drought Monitor (USDM) also used NDVI in monitoring droughts (Brown et al., 2008). A few recent publications have reported that water-related vegetation indices such as LSWI are relatively more sensitive to drought than greenness related VIs and presented as a potential drought monitoring tool (Chandrasekar et al., 2010; Gu et al., 2008; Wagle et al., 2015, 2014; Zhang et al., 2013). Long term analysis of LSWI over pluvial, dry and normal years can provide better insight into vegetation response to climate variations and complement current drought monitoring tools to incorporate water related vegetation index into their models and algorithms.

In this pilot and site-level study, we chose two tallgrass prairie sites in Oklahoma, which are the part of the Oklahoma Mesonet (McPherson et al., 2007). The objectives of this study were to: (a) explore the relationship between seasonal and inter-annual rainfall variability and dynamics of grassland vegetation growth, and (b) ascertain the sensitivity of VIs (NDVI, EVI and LSWI) to rainfall variations. This study further investigates additional drought information rendered by LSWI, based on episodic drought events over time series (2000–2013). Using the drought information generated from LSWI, a new approach (the number of days with LSWI < 0 during the plant growing season and LSWI-based drought severity classification) for an assessment of the drought impacts over grasslands is proposed in this study. This LSWI-based approach can potentially provide more insights into drought monitoring over tallgrass prairie grasslands.

Table 1
Drought indicators derived from several spectral indices, thermal products and precipitation.

Name of vegetation indices	Full name	Formula	References
1. Photosynthetic Indices (PIs)			
NDVI	Normalized difference vegetation index	$(\rho858 - \rho650)/(\rho858 + \rho650)$	Tucker (1979), Kogan (1991, 1995)
EVI	Enhanced vegetation index	$2.5 * (\rho858 - \rho650)/(\rho858 + 6 * \rho650 - 7 * \rho469 + 1)$	Huete et al. (2002), Saleska et al. (2007)
VCI	Vegetation condition index	$(NDVI - NDVI_{MIN})/(NDVI_{MAX} - NDVI_{MIN})$	Kogan (1995)
2. NIR and SWIR based indices			
$NDWI_{1240}$	Normalized Difference Water Index	$(\rho858 - \rho1240)/(\rho858 + \rho1240)$	Gao (1996)
LSWI	Land Surface Water Index	$(\rho858 - \rho1640)/(\rho858 + \rho1640)$	Xiao et al. (2002)
SWISI	Shortwave Infrared Water Stress Index	$(\rho1640 - \rho850)/(\rho1640 + \rho850)$ or $(\rho1240 - \rho850)/(\rho1240 + \rho850)$	Fensholt and Sandholt (2003)
$NDWI_{2130}$	Normalized Difference Water Index	$(\rho858 - \rho2130)/(\rho858 + \rho2130)$	Chen et al. (2005)
NMDI	Normalized Multiband Drought Index	$(\rho860 - (\rho1640 - \rho2130))/(\rho860 + (\rho1640 - \rho2130))$	Wang and Qu (2007)
3. Combined indices (PIs, LST and precipitation)			
VTCI	Vegetation Temperature Condition Index	NDVI, Land Surface Temperature (LST)	Moran et al. (1994), Wan et al. (2004)
TVDI	Temperature Vegetation Dryness Index	NDVI, LST	Sanholt et al. (2002)
SDCI	Scaled Drought Condition Index	LST, NDVI, Precipitation	Rhee et al. (2010)
VCI	Vegetation Condition Index	$(NDVI - NDVI_{MIN})/(NDVI_{MAX} - NDVI_{MIN})$	Kogan (1995)
NDDI	Normalized Difference Drought Index	$(NDVI - NDWI)/(NDVI + NDWI)$	Gu et al. (2007)

2. Materials and methods

2.1. Site description

The Marena site is located near Stillwater, OK (97.21694°W, 36.063493°N). This site is collocated with the Marena Oklahoma In-Situ Sensor Test bed (MOISST), a core calibration/validation site for NASA's soil moisture active passive (SMAP) satellite mission. The site contains relatively homogenous distribution of tallgrass prairie in sandy clay loam soil with similar grazing management practices over the years.

The El Reno site is located near El Reno, OK (98.0401°W, 35.5465°N) at the United States Department of Agriculture–Agriculture Research Service (USDA–ARS) Grazing Research laboratory (GRL). The site is an open terrain, slightly sloped from east to west and is covered by natural tallgrass prairie in silty clay loam soil. The location and the landscape features of the study sites are shown in Fig. 1 while the biophysical features of the sites are presented in Table 2.

2.2. Rainfall and soil moisture data during 2000–2013 from the Oklahoma Mesonet

The Oklahoma Mesonet is a system designed to measure the environmental parameters by a network of instruments deployed on or near a 10 m tall tower. The recorded measurements are aggregated into observations every five minutes and the observations are sent out to a central facility every five minutes, 24 h per day year-round (McPherson et al., 2007). Daily precipitation and soil moisture data from 2000–2013 at the Oklahoma Mesonet Marena and El Reno stations were downloaded from the Oklahoma Mesonet website (http://www.mesonet.org/index.php/weather/daily_data_retrieval). The daily data were aggregated into 8-day periods to match with the temporal resolution of the Moderate-Resolution Imaging Spectroradiometer (MODIS) derived VIs. Three different soil moisture data products (soil water potential, fractional water index and volumetric water content) are available at the Mesonet website. These soil moisture data products were derived based on the calibrated change in soil temperature over time after a heat pulse is introduced (Illston et al., 2008). In our analysis, we used volumetric soil water content (SWC) collected at three different soil profiles (5, 25, and 60 cm depth). The SWC measured by Mesonet is a point measurement, but it is representative from a magnitude and temporal variability standpoint at scales of up too several hundred meters or field scale (Basara and Crawford, 2002; Illston et al., 2008).

2.3. MODIS images and vegetation indices during 2000–2013

Daily images are acquired by the MODIS sensors on-board the Terra and Aqua satellites. Seven spectral bands: red (620–670 nm), NIR_1 (841–876 nm), blue (459–479 nm), green (545–565 nm), NIR_2 (1230–1250 nm), $SWIR_1$ (1628–1652 nm), and $SWIR_2$ (2105–2155 nm) are available for the study of vegetation. In this study, we used the 8-day composite land surface reflectance (MOD09A1) data from February 2000 to December 2013 for one

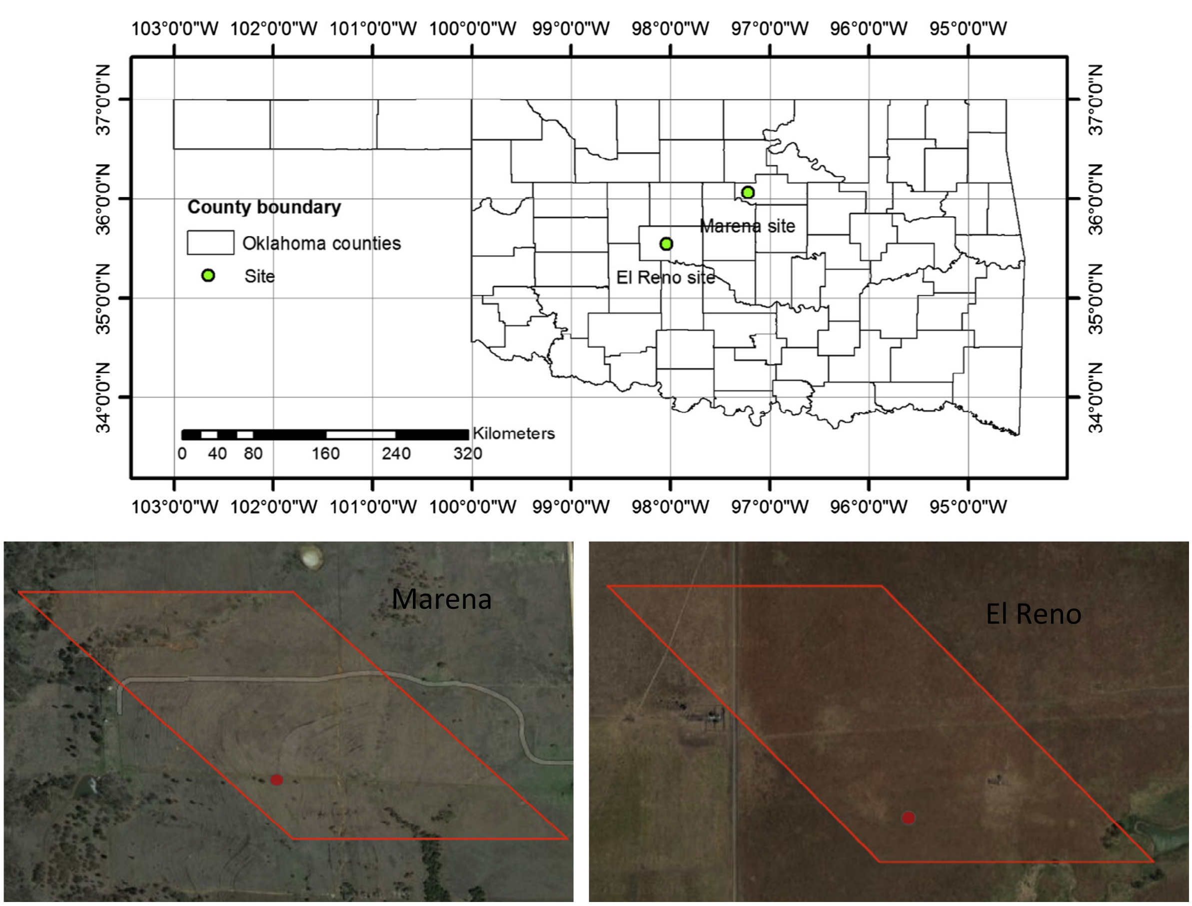

Fig. 1. The location (Oklahoma map) and the landscape features of the study sites. The red boarder line represents the size of a MODIS pixel at 500-m spatial resolution. (For interpretation of the references to colour in this figure legend, the reader is referred to the web version of this article.)

Table 2
Overview of the study sites.

Site	Latitude	Longitude	Elevation (m)	Mean annual rainfall (mm)	Mean annual temperature (°C)	Major vegetation	Soil type
Marena	36.063493 °N	97.2169 °W	327	802	14	Tallgrass prairie	Sandy clay loam
El Reno	35.5465 °N	98.0401°W	419	794	15	Tallgrass prairie	Silty clay loam

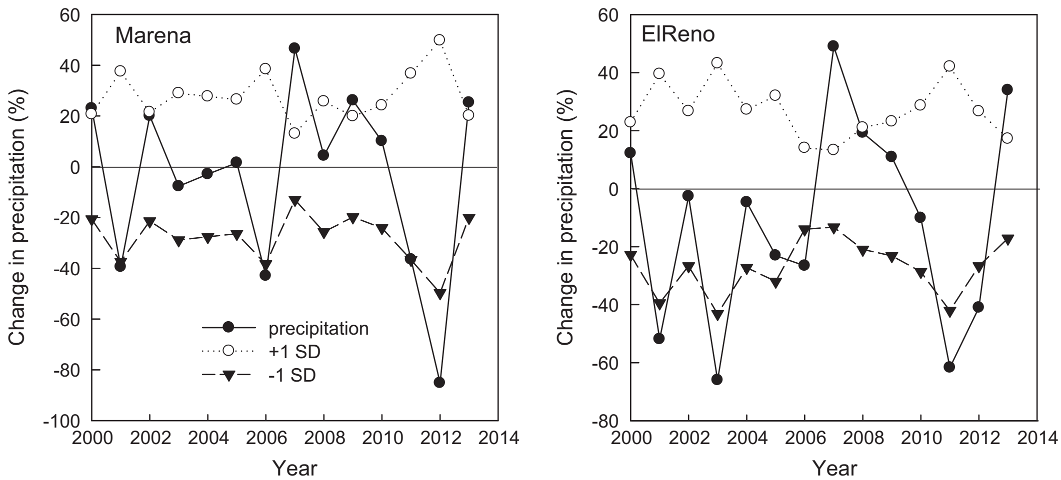

Fig. 2. The variability of annual rainfall at study sites over time (2000–2013). The anomaly of rainfall is calculated as percentage change from a 14-year average rainfall.

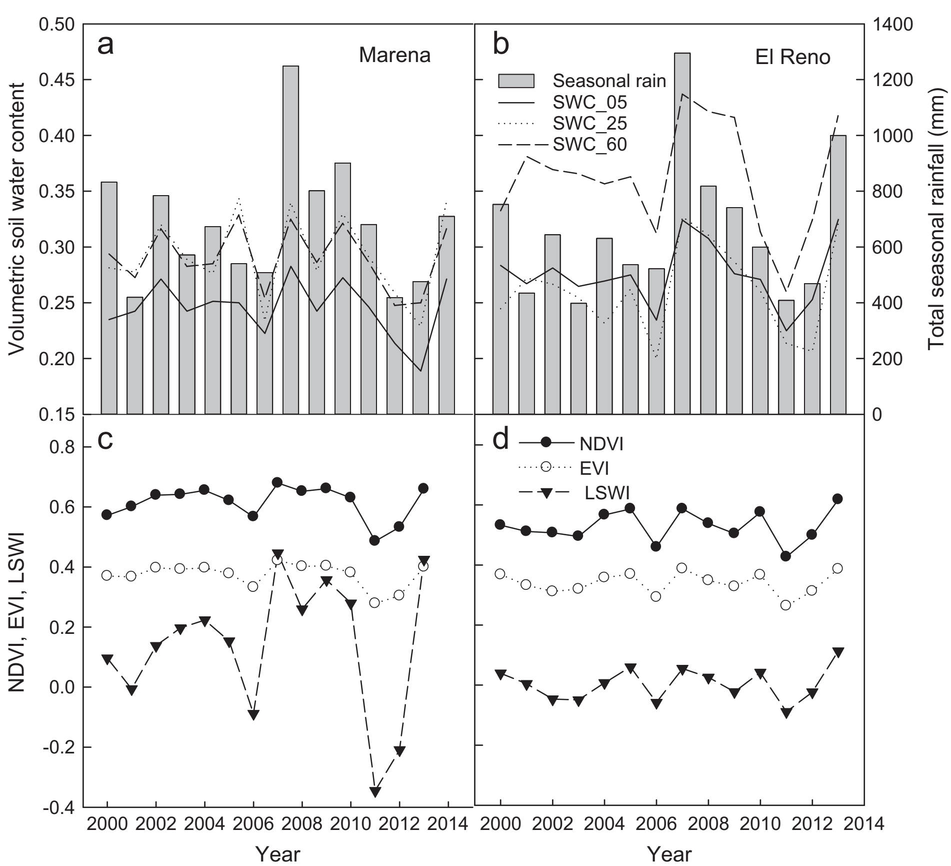

Fig. 3. Inter-annual variation of: soil water content at different soil depths (a and b) and growing season (March–October) vegetation indices (c and d). The vertical bars represent the total growing season rainfall.

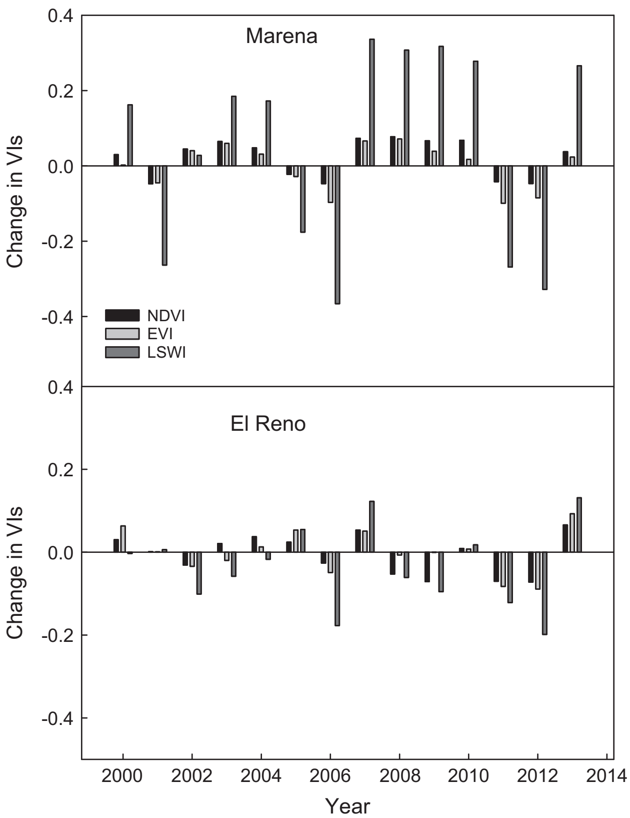

Fig. 4. Sensitivity analysis of three vegetation indices (NDVI, EVI, and LSWI) to drought. The change in absolute values of vegetation indices (maximum values) is computed based on 14-year average values deviated from mean.

MODIS pixel (500 m × 500 m spatial resolution) centered on the study sites. The dataset was extracted from the data portal at the Earth Observation and Modeling Facility (EOMF) at the University of Oklahoma (http://eomf.ou.edu/visualization/gmap/). Land surface reflectance (ρ) from blue, green, red, NIR_1, and $SWIR_1$ bands were used to calculate three spectral indices as follows:

$$\mathrm{NDVI} = \frac{\rho\mathrm{NIR1} - \rho\mathrm{red}}{\rho\mathrm{NIR1} + \rho\mathrm{red}} \tag{1}$$

$$\mathrm{EVI} = \frac{\rho\mathrm{NIR1} - \rho\mathrm{red}}{\rho\mathrm{NIR1} + 6 * \rho\mathrm{red} - 7.5\rho\mathrm{blue} + 1} \tag{2}$$

$$\mathrm{LSWI} = \frac{\rho\mathrm{NIR1} - \rho\mathrm{SWIR1}}{\rho\mathrm{NIR1} + \rho\mathrm{SWIR1}} \tag{3}$$

To understand the relative sensitivity of these three VIs to drought, we computed the deviation (absolute values) of the maximum values ($NDVI_{max}$, EVI_{max}, and $LSWI_{max}$) of VIs each year with reference to 14-year mean maximum VIs.

2.4. United states drought monitoring (USDM) data

The USDM is a composite drought index that includes many indicators based on measurements of climatic, hydrologic and soil conditions in order to provide weekly maps of drought conditions (Svoboda et al., 2002). The drought categories (D0, D1, D2, D3 and D4) for the study sites were extracted from the weekly drought maps published by the USDM (http://droughtmonitor.unl.edu/MapsAndData/). The corresponding NDVI and LSWI values to the USDM defined drought categories were identified from MODIS data and plotted against each other to define the LSWI-based drought classifications. This relationship between the USDM classified drought categories and MODIS-derived VIs were analyzed only for the Summer months (June–August) of each year from 2000–2013.

3. Results

3.1. Inter-annual variation of rainfall, soil water content and vegetation indices-identifying drought years

Annual precipitation varied substantially during 2000–2013 at both sites with an annual average precipitation of 802 mm (±220) at the Marena site and 794 mm (±182) at the El Reno site. Dry and pluvial years were determined based on the 14-year (2000–2013) average annual precipitation and the associated standard deviation. Years with standardized score values greater than

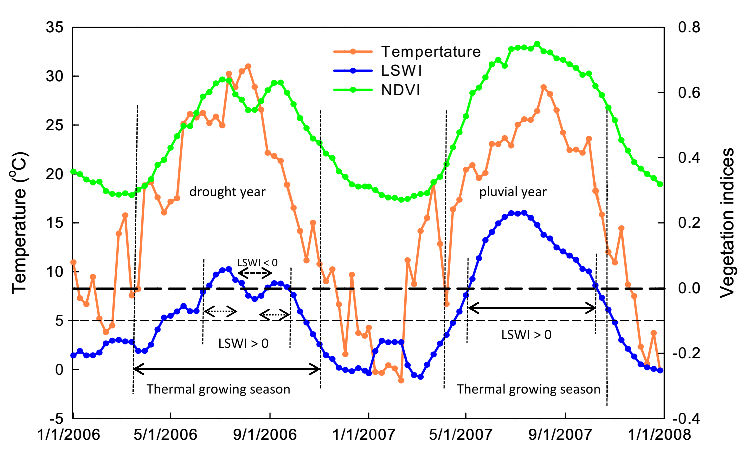

Season	Months	LSWI values	Drought
spring	Mar-May	if LSWI < 0 after green-up during April- May	spring drought
summer	Jun-Aug	if LSWI < 0 during Jun-Aug	summer drought
fall	Sep-Nov	if LSWI < 0 during Sep-Oct before senescence	fall drought

Fig. 5. Schematic diagram showing seasonal dynamics of air temperature, NDVI and LSWI in drought (2006) and non-drought year (2007). The inset table (below) presents the designation of drought types based on LSWI values and seasons.

sum of its average and one standard deviation (negative side) were labeled as drought years, whereas years with standardized score greater than sum of its average and one standard deviation (positive side) were identified as pluvial years (Fig. 2). From this analysis, the years 2001, 2006, 2011, and 2012 were identified as drought years at both Marena and El Reno sites. In addition, 2003 also was a drought year at the El Reno site. Additionally, 2007 and 2013 were identified as pluvial years for both sites. For both sites, two episodic drought years (2006 and 2012) were compared with two episodic pluvial years (2007 and 2013).

Fig. 3(a) and (b) shows SWC at various depths (5, 25, and 60 cm). The growing season average SWC of drought years (2006 and 2012) was approximately 20–25% (5 and 25 cm depths) and 25–30% at 60 cm whereas SWC at three depths ranged from 27% to 44% in pluvial years (2012 and 2013). At El Reno, SWC at the 60 cm depth was relatively higher than that of Marena for all years.

Fig. 3(c) and (d) shows inter-annual variation of seasonal mean VIs (NDVI, EVI, and LSWI). NDVI and EVI had relatively smaller variations compared to the variation observed in LSWI. The average NDVI, EVI and LSWI values during the growing season were consistently lower ($NDVI_{avg} < 0.55$, $EVI_{avg} < 0.35$ and $LSWI_{avg} < 0$) in drought years (2006 and 2012) in comparison with pluvial years (2007 and 2013). Both sites showed consistently lower values of VIs in drought years. However, VIs at the Marena site were more sensitive to drought than those at the El Reno site.

To understand the relative sensitivity of VIs to drought, the deviation in the maximum values of VIs ($NDVI_{max}$, EVI_{max} and $LSWI_{max}$) for each year were compared to long term (2000–2013) mean of maximum VIs (Fig. 4). The largest negative LSWI anomaly was observed in drought years (2006 and 2012) at both sites, although the magnitudes of decrease varied between sites. LSWI showed the largest deviations in drought and pluvial years compared to NDVI and EVI. For Example, $LSWI_{max}$ was reduced by −0.36 (66%) and −0.32 (59%) at the Marena site, and by −0.18 (43%) and −0.2 (62%) at the El Reno site in 2006 and 2012, respectively. The change in EVI_{max} in drought years was greater than that of $NDVI_{max}$. In 2006 and 2012, drought reduced the EVI_{max} by almost two folds compared to $NDVI_{max}$. At the Marena site, the drought reduced $NDVI_{max}$ by −0.04 (7%) whereas EVI_{max} was reduced by −0.09 (17%) and −0.07 (14%) in 2006 and 2012,

Table 3
Summary of the start of growing season (SOS), ending of growing season (EOS), duration (in days) of land surface water index (LSWI < 0) during Spring and Summer for the study sites over the study period (2000–2013).

Year	Marena					El Reno				
	SOS ($T_{min} > 5$ °C)	Duration of LSWI < 0 (spring)	Duration of LSWI < 0 (summer)	Summer rainfall (mm)	EOS ($T_{min} < 5$ °C)	SOS ($T_{min} > 5$ °C)	Duration of LSWI < 0 (spring)	Duration of LSWI < 0 (summer)	Summer rainfall (mm)	EOS ($T_{min} < 5$ °C)
2000	21-March	24	10	394	07-October	21-March	42	0	250	05-October
2001	02-April	40	23	203	09-October	02-April	42	16	135	13-October
2002	10-April	40	8	281	11-October	06-April	56	24	151	10-October
2003	11-April	32	0	225	24-October	13-April	80	24	172	24-October
2004	15-April	16	0	312	29-October	15-April	56	8	283	02-November
2005	04-April	48	8	362	20-October	13-April	16	0	309	22-October
2006	29-March	56	53	164	17-October	29-March	56	40	214	17-October
2007	18-April	24	0	570	20-October	17-April	24	0	655	20-October
2008	16-April	24	0	297	14-October	20-April	24	0	356	21-October
2009	15-April	32	8	353	07-October	21-April	24	16	260	21-October
2010	10-April	16	8	265	27-October	10-April	24	0	314	25-October
2011	17-April	24	76	124	17-October	06-April	88	32	153	18-October
2012	11-March	56	34	191	24-October	11-March	72	42	102	24-October
2013	26-April	24	0	325	15-October	26-April	8	0	434	15-October

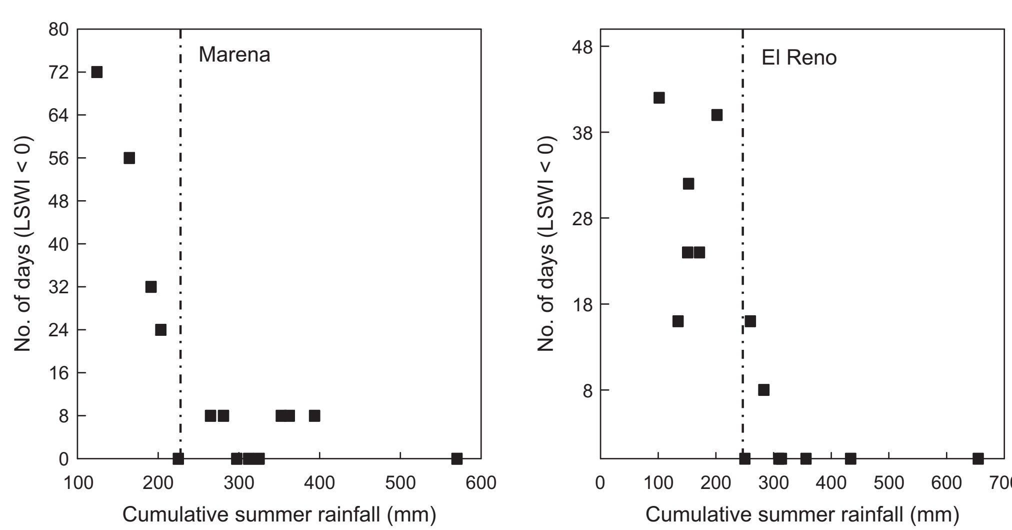

Fig. 6. Relationship between duration of negative LSWI and cumulative rainfall during summer (June–August). The vertical dashed lines intersecting the x-axis represent the summer rainfall thresholds.

respectively. Similarly at the El Reno site, $NDVI_{max}$ was reduced only by −0.02 (4%) and −0.06 (10%) whereas EVI_{max} was reduced by −0.04 (10%) and −0.09 (19%) in 2006 and 2012, respectively.

3.2. Seasonal dynamics of rainfall, soil water content and vegetation indices – identifying Spring drought and Summer drought within a year

Fig. 5 represents the schematic diagram of air temperature, NDVI, and LSWI dynamics during the drought and pluvial years. During pluvial years, the duration of LSWI > 0 period was longer and LSWI values were positive throughout the growing season. Air temperature over a certain threshold (>5 °C) in the spring determines the start of the growing season (late March-early April). After greening up in spring, the rate of vegetation growth depends on available SWC. If the plant available SWC is not sufficient then the vegetation experiences stress. As such, LSWI < 0 during the Mar-May period was designated as Spring drought. LSWI < 0 during the Summer period (June–August) was defined as Summer drought, while LSWI < 0 during the late growing season (September–October) was defined as Fall drought (Fig. 5 inset Table). Thus, a year could have Spring, Summer and/or Fall droughts as per the rainfall received for that period of that year.

Duration of negative LSWI (LSWI < 0) during summer (June, July and August) was longer in drought years than pluvial and normal years (Table 3). For example, LSWI values were negative for 56 and 42 days during summer months in 2006 at the Marena and El Reno sites, respectively. Further, LSWI values were negative for 72 days during the summer of 2011 at the Marena site. In contrast, LSWI values never fell below zero in the summer of pluvial years (2007 and 2013) at both sites. These results indicate the potential of LSWI to track water status of vegetation during dry summers. Interestingly, the duration of negative LSWI values during summer showed a definite pattern when plotted with the cumulative summer rainfall (Fig. 6). For those years with summer rainfall less than certain thresholds (230 mm for Marena site and 250 mm for El Reno site), duration of negative LSWI values increased linearly as the cumulative summer rainfall decreased. However, the relationship collapsed when the summer rainfall exceeded the threshold. The years with summer rainfall over the threshold had zero or only one 8-day period with LSWI < 0.

The relationship between NDVI and LSWI for summer months (June–August) over the 14-years is presented in Fig. 7. Each point in the plot represents the weekly observation of drought severity designation for the study area as determined from USDM drought maps (http://droughtmonitor.unl.edu/MapsAndData/). The descriptions of the drought intensity defined by the USDM are listed Fig. 7 inset table. Results illustrated that VIs values were much lower (NDVI < 0.6 and LSWI < 0) during higher intensity droughts, identified as D2, D3 and D4 by the USDM, whereas NDVI and LSWI values were higher (NDVI > 0.6 and LSWI > 0) in lower intensity and non-drought conditions, identified as D1 (moderate) and D0 (dry) by the USDM. Based on LSWI values during the summer months, drought was classified into non-drought or dry (LSWI > 0.1), moderate (0 < LSWI ⩽ 0.1), severe (−0.1 < LSWI ⩽ 0) and extreme-exceptional drought (LSWI ⩽ −0.1) corresponding to USDM's 0 or D0, D1, D2 and D3 or D4 categories, respectively.

4. Discussions

Globally, all ecosystems will be impacted to a greater extent by the climatic extremes in future because most of the global climate models predicted more extremes in the climates such as multi-year droughts (Field et al., 2014). Previous studies reported the sensitivity of the U.S. Southern Great Plains grassland to extreme drought events during the historic droughts of the 1930s and 1950s (Albertson et al., 1957; Albertson and Weaver, 1944). Both pure and mixed prairies were seriously depleted by those historic droughts and a long delay occurred in the recovery of the vegetation. The negative impacts of two episodic droughts of 2006 and 2012 over tallgrass prairie were apparent in our study as documented by the lower values of NDVI, EVI and LSWI (Fig. 3). Sensitivity of grassland vegetation to drought, when monitored through several VIs, showed varied degrees of response. LSWI

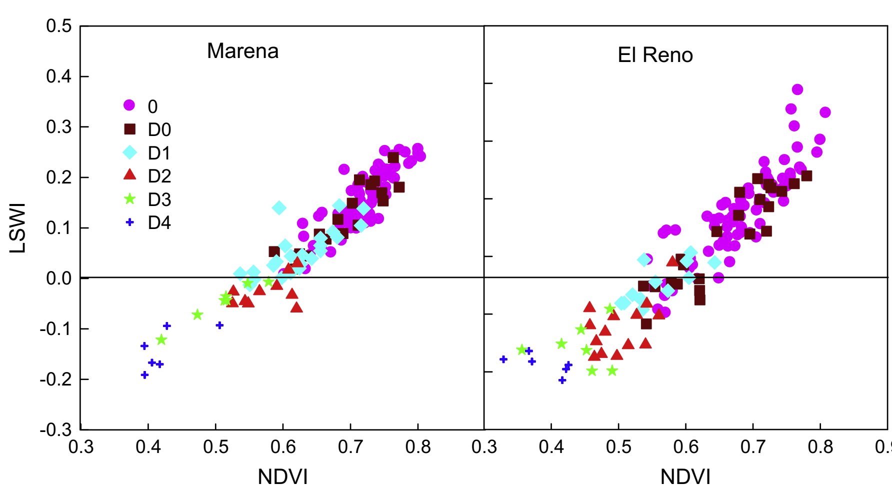

Drought Class	Description	PDSI	LSWI-D values and drought class
0 D0	non-drought abnormally dry	-0.49 or more -0.5 to -1.99	LSWI > 0.1
D1	drought-moderate	-2.0 to -2.99	0 <LSWI ≤ 0.1
D2	drought-severe	-3.0 to -3.99	-0.1 < LSWI ≤ 0
D3 D4	drought-extreme drought- exceptional	-4.0 or less	LSWI ≤ -0.1

Fig. 7. Relationship between: NDVI and LSWI for individual pixels of the grassland study sites for June–August over a 14-year study period (2000–2013). Drought severity categories defined by USDM, Palmer Drought Severity Index (PDSI) and LSWI-based drought categories (inset table).

was the most sensitive indicator of vegetation condition followed by EVI and NDVI. For example, $NDVI_{max}$ was 0.63 (7% less than 14-year average, 0.69), the EVI_{max} was 0.39 in 2012 (14% less than 14-year average, 0.45) and the $LSWI_{max}$ was 0.22 (59% less than 14-year average, 0.56) in 2012 at the Marena site.

Years with abundant rainfall (2007 and 2013) were characterized by the positive LSWI throughout the entire season, while LSWI values decreased below zero and remained negative during the summer droughts in 2006 and 2012. This finding is in agreement with the results reported by Wagle et al. (2014) for El Reno tallgrass prairie sites in Oklahoma. The sharper drop in LSWI values in drought years revealed that the grassland vegetation had lost a greater amount of water than the greenness because loss of chlorophyll and leaves is a rather slow process compared to water loss from stomata via transpiration during drought (Chaves et al., 2003). Therefore, LSWI can give a stronger vegetation drought signal than that of NDVI or EVI. Chandrasekar et al. (2010) also reported that LSWI responded more directly to the water status of the vegetation than did NDVI and EVI. Negative LSWI during the summer not only indicated the drought but also reflected the relative persistency of summer droughts. The longer the period of LSWI < 0, the lesser the amount of rainfall was received by the ecosystem and vice versa, indicating relative drought persistency or duration (Fig. 6). For example, LSWI < 0 in 2011 (Marena site) lasted for a longer period than in 2006 (72 and 32 days, respectively), which indicates more persistent summer drought in 2011 than in 2006. Rainfall events correlate with the soil moisture regimes and LSWI being the sensitive index provided an earlier signal of declining SWC than did NDVI and EVI. For instance, at the Marena site, LSWI dropped below zero indicating droughts during late June (DOY 170) of 2006 (Fig. 8e) when the SWC dropped below 12% whereas the NDVI reduced late during mid-July (DOY 200) only when SWC dropped below 12% for a substantial period of time (Fig. 8a). However, most of the models and drought monitoring

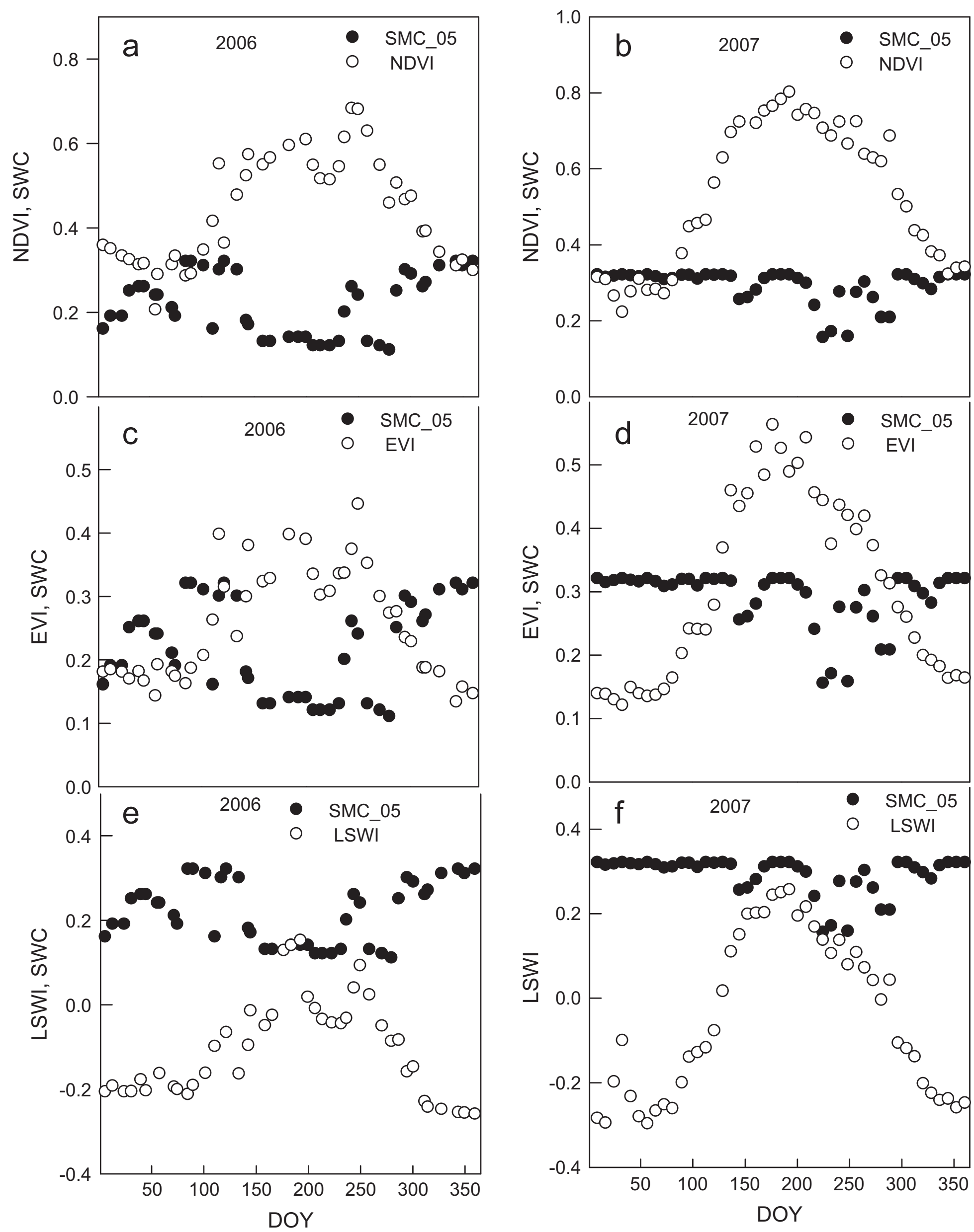

Fig. 8. Seasonal soil moisture dynamics between dry and wet years and sensitivity of NDVI (a and b) EVI (c and d) and LSWI (e and f) to declining soil moisture at the 5 cm depth (Marena).

algorithms for the last two decades (Hartmann et al., 2003; Ji and Peters, 2003; Liu and Kogan, 1996; Nemani and Running, 1989; Pettorelli et al., 2005) have widely used NDVI as a drought index.

Updating the climate based drought indicators such as Palmer Drought Severity Index (PDSI) and Standardized Precipitation Index (SPI), USDM has introduced the VegDRI in 2007 (Brown et al., 2008). This drought-monitoring indicator provides a measure of drought severity by integrating satellites observation, local weather report and experts reviews. The USDM employs NDVI observations that are more characteristic features of plant greenness and was found to be relatively less sensitive to drought compared to EVI and LSWI in our study. Our study (14 years) over the grassland based on sensitivity of VIs to past drought revealed that LSWI could not only monitor the drought occurrence but also designate drought into different intensity categories (Fig. 7). Traditionally, USDM has used PDSI to classify drought into different classes (D0, D1, D2, D3 and D4). Such climate based drought monitoring and classification approaches have coarse spatial resolutions and do not better represent vegetation status since the interpretation depends heavily on point based meteorological measurements (Brown et al., 2008). We attempted to describe drought severity categories quantitatively based on LSWI values of vegetation which is relatively more precise and useful because it is a pixel based finer resolution and vegetation specific calculation and is more related to water status of vegetation than greenness. The classification of drought categories are simply grouped based on two dimensional spaces of NDVI and LSWI plots where each point represents the weekly observation of drought severity designation for the study area as determined from USDM (Fig. 7). In our study, we found that higher negative values of LSWI represent a higher intensity drought. For example, when LSWI was -0.1 or smaller we defined it as extreme drought, comparable to D3 and D4 (extreme and exceptional) categories by USDM, while moderate-severe droughts were identified when LSWI values ranged greater or equal to zero to less than -0.1 corresponding to D1 and D2 drought categories of USDM classification. Overall, good vegetation growth exhibited higher LSWI values, which decreased with drought and ultimately became negative when drought became more extreme. Therefore, by using the information rendered by LSWI during the drought, we can quantitatively investigate the drought impacts on vegetation that can contribute toward the development of more robust tools for monitoring drought stress in vegetation.

5. Conclusion

We used 14 years of MODIS-derived VIs, Mesonet soil moisture and rainfall data at Marena and El Reno tallgrass prairie sites to study the impact of drought events on grassland phenology and growth through analyzing sensitivity differences of vegetation indices to drought. Specifically, the drought events (2006 and 2012) that occurred in the last 14 years negatively impacted the growth of the vegetation. When three VIs were compared, LSWI decreased the most in drought years followed by EVI and NDVI, indicating that LSWI was the most sensitive indicator to the drought events. The number of days with LSWI < 0 was found higher during the summer droughts of 2006 and 2012, showing the ability of LSWI to track drought. Based on this finding, a new approach of drought assessment, counting number of days with LSWI < 0 and LSWI-based drought severity classification, is proposed in this study. LSWI values were more negative for the period of intensity drought categories (D2, D3 and D4) defined by USDM, demonstrating that LSWI could be used to describe the hydrological condition of the tallgrass prairie as an effective additional VI for drought assessment. However, a more thorough evaluation of this approach as a drought monitoring tool for widely distributed grasslands and other vegetation types is required and will be the subject of future research.

Acknowledgements

This study was supported in part by a research grant (Project No. 2012-02355) through the USDA National Institute for Food and Agriculture (NIFA)'s Agriculture and Food Research Initiative (AFRI), Regional Approached for Adaptation and Mitigation of Climate Variability and Change grant (IIA-1301789), and NOAA Climate Office's Sectoral Applications Research Program (SRP) grant NA130AR4310122. We would also like to thank Cory B. Northern for the English correction and manuscript editing.

References

Albertson, F., Tomanek, G., Riegel, A., 1957. Ecology of drought cycles and grazing intensity on grasslands of central Great Plains. Ecol. Monographs, 27–44.
Albertson, F., Weaver, J., 1944. Nature and degree of recovery of grassland from the great drought of 1933 to 1940. Ecol. Monogr. 14, 393–479.
Basara, J.B., Crawford, K.C., 2002. Linear relationships between root-zone soil moisture and atmospheric processes in the planetary boundary layer. J. Geophys. Res.: Atmospheres (1984–2012) 107 (ACL 10–11-ACL 10–18).
Basara, J.B., Maybourn, J.N., Peirano, C.M., Tate, J.E., Brown, P.J., Hoey, J.D., Smith, B.R., 2013. Drought and Associated Impacts in the Great Plains of the United States—A Review.
Bhalme, H., Reddy, R., Mooley, D., Murty, B.V.R., 1981. Solar activity and Indian weather/climate. Proc. Indian Acad. Sci.-Earth Planetary Sci. 90, 245–262.
Boschetti, M., Nutini, F., Brivio, P.A., Bartholomé, E., Stroppiana, D., Hoscilo, A., 2013. Identification of environmental anomaly hot spots in West Africa from time series of NDVI and rainfall. ISPRS J. Photogrammetry Remote Sens. 78, 26–40.
Brown, J.F., Wardlow, B.D., Tadesse, T., Hayes, M.J., Reed, B.C., 2008. The vegetation drought response index (VegDRI): a new integrated approach for monitoring drought stress in vegetation. GISci. Remote Sens. 45, 16–46.
Ceccato, P., Flasse, S., Tarantola, S., Jacquemoud, S., Grégoire, J.-M., 2001. Detecting vegetation leaf water content using reflectance in the optical domain. Remote Sens. Environ. 77, 22–33.
Chandrasekar, K., Sesha Sai, M., Roy, P., Dwevedi, R., 2010. Land surface water index (LSWI) response to rainfall and NDVI using the MODIS vegetation index product. Int. J. Remote Sens. 31, 3987–4005.
Chaves, M.M., Maroco, J.P., Pereira, J.S., 2003. Understanding plant responses to drought—from genes to the whole plant. Funct. Plant biol. 30, 239–264.
Chen, D., Huang, J., Jackson, T.J., 2005. Vegetation water content estimation for corn and soybeans using spectral indices derived from MODIS near-and short-wave infrared bands. Remote Sens. Environ. 98, 225–236.
Christian, J., Christian, K., Basara, J.B., 2015. Drought and pluvial dipole events within the great plains of the United States. J. Appl. Meteorol. Climatol.
Diodato, N., Bellocchi, G., 2008. Modelling vegetation greenness responses to climate variability in a Mediterranean terrestrial ecosystem. Environ. Monit. Assess. 143, 147–159.
Fensholt, R., Sandholt, I., 2003. Derivation of a shortwave infrared water stress index from MODIS near-and shortwave infrared data in a semiarid environment. Remote Sens. Environ. 87, 111–121.
Field, C.B., Barros, V.R., Mach, K., Mastrandrea, M., 2014. Climate change 2014: impacts, adaptation, and vulnerability. Contribution of Working Group II to the Fifth Assessment Report of the Intergovernmental Panel on Climate Change.
Gao, B.-C., 1996. NDWI—a normalized difference water index for remote sensing of vegetation liquid water from space. Remote Sens. Environ. 58, 257–266.
Ghulam, A., Li, Z.-L., Qin, Q., Tong, Q., 2007. Exploration of the spectral space based on vegetation index and albedo for surface drought estimation. J. Appl. Remote Sens. 1, 013529-013529-013512.
Gu, Y., Brown, J.F., Verdin, J.P., Wardlow, B., 2007. A five-year analysis of MODIS NDVI and NDWI for grassland drought assessment over the central Great Plains of the United States. Geophys. Res. Lett. 34.
Gu, Y., Hunt, E., Wardlow, B., Basara, J.B., Brown, J.F., Verdin, J.P., 2008. Evaluation of MODIS NDVI and NDWI for vegetation drought monitoring using Oklahoma Mesonet soil moisture data. Geophys. Res. Lett. 35.
Hardisky, M.A., Klemas, V., Smart, R.M., 1983. The influence of soil salinity, growth form, and leaf moisture on the spectral radiance of *Spartina alterniflora* canopies. Photogramm. Eng. Rem. Sens. 49, 77–83.
Hartmann, T., Di Bella, C., Oricchio, P., 2003. Assessment of the possible drought impact on farm production in the SE of the province of Buenos Aires, Argentina. ISPRS J. Photogrammetry Remote Sens. 57, 281–288.
Herrmann, S.M., Anyamba, A., Tucker, C.J., 2005. Exploring relationship between rainfall and vegetation dynamics in the Sahel using coarse resolution satellite data. STATEMENT BY THE AUTHOR, 79.
Hollinger, S., Isard, S., Welford, M., 1993. A new soil moisture drought index for predicting crop yields. In: Preprints, Eighth Conference on Applied Climatology. pp. 187–190.

Huete, A., Didan, K., Miura, T., Rodriguez, E.P., Gao, X., Ferreira, L.G., 2002. Overview of the radiometric and biophysical performance of the MODIS vegetation indices. Remote Sens. Environ. 83, 195–213.
Hunt, E.R., Rock, B.N., 1989. Detection of changes in leaf water content using near- and middle-infrared reflectances. Remote Sens. Environ. 30, 43–54.
Illston, B.G., Basara, J.B., Fiebrich, C.A., Crawford, K.C., Hunt, E., Fisher, D.K., Elliott, R., Humes, K., 2008. Mesoscale monitoring of soil moisture across a statewide network. J. Atmos. Oceanic Technol. 25, 167–182.
Jackson, T.J., Chen, D., Cosh, M., Li, F., Anderson, M., Walthall, C., Doriaswamy, P., Hunt, E.R., 2004. Vegetation water content mapping using Landsat data derived normalized difference water index for corn and soybeans. Remote Sens. Environ. 92, 475–482.
Ji, L., Peters, A.J., 2003. Assessing vegetation response to drought in the northern Great Plains using vegetation and drought indices. Remote Sens. Environ. 87, 85–98.
Kimes, D., Markham, B., Tucker, C., McMurtrey, J., 1981. Temporal relationships between spectral response and agronomic variables of a corn canopy. Remote Sens. Environ. 11, 401–411.
Kogan, F., 1991. Observations of the 1990 US drought from the NOAA-11 polar-orbiting satellite. Drought Netw. News 3, 7–11.
Kogan, F., 1995. Application of vegetation index and brightness temperature for drought detection. Adv. Space Res. 15, 91–100.
Liu, W., Kogan, F., 1996. Monitoring regional drought using the vegetation condition index. Int. J. Remote Sens. 17, 2761–2782.
Maki, M., Ishiahra, M., Tamura, M., 2004. Estimation of leaf water status to monitor the risk of forest fires by using remotely sensed data. Remote Sens. Environ. 90, 441–450.
McKee, T.B., Doesken, N.J., Kleist, J., 1993. The relationship of drought frequency and duration to time scales. In: Proceedings of the 8th Conference on Applied Climatology. American Meteorological Society, Boston, MA, pp. 179–183.
McPherson, R.A., Fiebrich, C.A., Crawford, K.C., Kilby, J.R., Grimsley, D.L., Martinez, J.E., Basara, J.B., Illston, B.G., Morris, D.A., Kloesel, K.A., 2007. Statewide monitoring of the mesoscale environment: a technical update on the Oklahoma Mesonet. J. Atmos. Oceanic Technol. 24, 301–321.
Moran, M., Clarke, T., Inoue, Y., Vidal, A., 1994. Estimating crop water deficit using the relation between surface-air temperature and spectral vegetation index. Remote Sens. Environ. 49, 246–263.
Narasimhan, B., Srinivasan, R., 2005. Development and evaluation of soil moisture deficit index (SMDI) and evapotranspiration deficit index (ETDI) for agricultural drought monitoring. Agric. For. Meteorol. 133, 69–88.
Nemani, R.R., Running, S.W., 1989. Estimation of regional surface resistance to evapotranspiration from NDVI and thermal-IR AVHRR data. J. Appl. Meteorol. 28, 276–284.
Oklahoma Water Resources Board, 2010. Oklahoma Comprehensive Water Plan Supplemental Report-Climate Issues and Recommendations, last accessed March, 2015 at https://www.owrb.ok.gov/supply/ocwp/pdf_ocwp/WaterPlanUpdate/draftreports/OCWP_Climate_IssuesReccs.pdf.
Palmer, W.C., 1965. Meteorological drought. US Department of Commerce, Weather Bureau Washington, DC, USA.
Peters, A.J., Walter-Shea, E.A., Ji, L., Vina, A., Hayes, M., Svoboda, M.D., 2002. Drought monitoring with NDVI-based standardized vegetation index. Photogrammetric Eng. Remote Sens. 68, 71–75.
Pettorelli, N., Vik, J.O., Mysterud, A., Gaillard, J.-M., Tucker, C.J., Stenseth, N.C., 2005. Using the satellite-derived NDVI to assess ecological responses to environmental change. Trends Ecol. Evol. 20, 503–510.
Qin, Y., Xiao, X., Dong, J., Zhou, Y., Zhu, Z., Zhang, G., Du, G., Jin, C., Kou, W., Wang, J., 2015. Mapping paddy rice planting area in cold temperate climate region through analysis of time series Landsat 8 (OLI), Landsat 7 (ETM+) and MODIS imagery. ISPRS J. Photogrammetry Remote Sens. 105, 220–233.
Reichstein, M., Tenhunen, J.D., Roupsard, O., Ourcival, J.m., Rambal, S., Miglietta, F., Peressotti, A., Pecchiari, M., Tirone, G., Valentini, R., 2002. Severe drought effects on ecosystem CO_2 and H_2O fluxes at three Mediterranean evergreen sites: revision of current hypotheses? Glob. Change Biol. 8, 999–1017.
Rhee, J., Im, J., Carbone, G.J., 2010. Monitoring agricultural drought for arid and humid regions using multi-sensor remote sensing data. Remote Sens. Environ. 114, 2875–2887.
Shafer, B., Dezman, L., 1982. Development of a Surface Water Supply Index (SWSI) to assess the severity of drought conditions in snowpack runoff areas. In: Proceedings of the Western Snow Conference. pp. 164–175.
Saleska, S.R., Didan, K., Huete, A.R., Da Rocha, H.R., 2007. Amazon forests green-up during 2005 drought. Science 318, 612.
Sandholt, I., Rasmussen, K., Andersen, J., 2002. A simple interpretation of the surface temperature/vegetation index space for assessment of surface moisture status. Remote Sens. Environ. 79, 213–224.
Song, Y., Ma, M., 2011. A statistical analysis of the relationship between climatic factors and the normalized difference vegetation index in China. Int. J. Remote Sens. 32, 3947–3965.
Svoboda, M., LeComte, D., Hayes, M., Heim, R., Gleason, K., Angel, J., Rippey, B., Tinker, R., Palecki, M., Stooksbury, D., 2002. The drought monitor. Bull. Am. Meteorol. Soc. 83, 1181–1190.
Tadesse, T., Brown, J.F., Hayes, M.J., 2005. A new approach for predicting drought-related vegetation stress: integrating satellite, climate, and biophysical data over the US central plains. ISPRS J. Photogrammetry Remote Sens. 59, 244–253.
Tucker, C.J., 1979. Red and photographic infrared linear combinations for monitoring vegetation. Remote Sens. Environ. 8, 127–150.
Tucker, C.J., 1980. Remote sensing of leaf water content in the near infrared. Remote Sens. Environ. 10, 23–32.
Van Rooy, M., 1965. A rainfall anomaly index independent of time and space. Notos 14, 43–48.
Wagle, P., Xiao, X., Suyker, A.E., 2015. Estimation and analysis of gross primary production of soybean under various management practices and drought conditions. ISPRS J. Photogrammetry Remote Sens. 99, 70–83.
Wagle, P., Xiao, X., Torn, M.S., Cook, D.R., Matamala, R., Fischer, M.L., Jin, C., Dong, J., Biradar, C., 2014. Sensitivity of vegetation indices and gross primary production of tallgrass prairie to severe drought. Remote Sens. Environ. 152, 1–14.
Wan, Z., Wang, P., Li, X., 2004. Using MODIS land surface temperature and normalized difference vegetation index products for monitoring drought in the southern Great Plains, USA. Int. J. Remote Sens. 25, 61–72.
Wang, J., Price, K., Rich, P., 2001. Spatial patterns of NDVI in response to precipitation and temperature in the central Great Plains. Int. J. Remote Sens. 22, 3827–3844.
Wang, L., Qu, J.J., 2007. NMDI: A normalized multi-band drought index for monitoring soil and vegetation moisture with satellite remote sensing. Geophys. Res. Lett. 34.
Weghorst, K., 1996. The reclamation drought index: guidelines and practical applications. In: North American Water and Environment Congress & Destructive Water. ASCE, pp. 637–642.
Weiying, C., Qianguang, X., Yongwei, S., 1994. Application of the anomaly vegetation index to monitoring heavy drought in 1992. Remote Sens. Environ. 9, 106–112.
Wilhite, D.A., Glantz, M.H., 1985. Understanding: the drought phenomenon: the role of definitions. Water Int. 10, 111–120.
Xiao, X., Boles, S., Liu, J., Zhuang, D., Liu, M., 2002. Characterization of forest types in Northeastern China, using multi-temporal SPOT-4 VEGETATION sensor data. Remote Sens. Environ. 82, 335–348.
Yang, L., Wylie, B.K., Tieszen, L.L., Reed, B.C., 1998. An analysis of relationships among climate forcing and time-integrated NDVI of grasslands over the US northern and central Great Plains. Remote Sens. Environ. 65, 25–37.
Zhang, G., Xiao, X., Dong, J., Kou, W., Jin, C., Qin, Y., Zhou, Y., Wang, J., Menarguez, M.A., Biradar, C., 2015. Mapping paddy rice planting areas through time series analysis of MODIS land surface temperature and vegetation index data. ISPRS J. Photogrammetry Remote Sens. 106, 157–171.
Zhang, N., Hong, Y., Qin, Q., Liu, L., 2013. VSDI: a visible and shortwave infrared drought index for monitoring soil and vegetation moisture based on optical remote sensing. Int. J. Remote Sens. 34, 4585–4609.